Supporting Information

Imoto et al. 10.1073/pnas.1303483110

SI Text

Synchronization and Isolation of Dividing Peroxisome Fraction. *Cyanidioschyzon merolae* 10D was used in this study (1). *C. merolae* was cultured in flasks, with shaking, under continuous light (40 W/m^2) at 42 °C. For synchronization, cell cultures were subcultured to $<1 \times 10^7$ cells/mL in a flat-bottom flask and subjected to a 12-h light/12-h dark cycle at 42 °C using an automatic light/dark cycle CM incubator (Fujimotorika) (2). Synchronized cells were treated with a 1/2,500 volume of 100 mM oryzalin stock solution dissolved in dimethyl sulfoxide after 8 h of the second light period. Cells were harvested at 12 h after the oryzalin treatment (late M phase). Cells were collected after centrifugation at 750 × *g* for 5 min and incubated at 42 °C in the dark for 40 min in isolation medium [20 mM Tris·HCl (pH 7.6), 5 mM $MgCl_2$, 5 mM KCl, 5 mM EGTA] containing 180 mM sucrose, 40 mM oryzalin (hypotonic isolation medium), and 3 mg/mL Complete EDTA-free protease inhibitor mixture (Roche). Next, cells (2×10^8 cells per milliliter) were lysed in a French Pressure Cell (SLM/Aminco) at 600 psi. After addition of 100 μg/mL DNase I and 0.5% wt/vol Triton X-100, the lysate was incubated for 1 h on ice and then layered on a three-step Percoll gradient in 40-mL tubes [10 mL of 60% (vol/vol), 10 mL of 40% (vol/vol), and 4 mL of 20% (vol/vol) Percoll dissolved in isolation medium containing 300 mM sucrose (isotonic isolation medium)]. After centrifugation at 23,000 × *g* for 50 min in a swinging-bucket rotor (P28S; Hitachi Koki), the fraction at the 40% Percoll interface was incubated in isotonic isolation medium containing 2% wt/vol Triton X-100 for 2 h on ice and then layered on a four-step Percoll gradient in 40-mL tubes [5 mL of 40% (vol/vol), 5 mL of 25% (vol/vol), 10 mL of 10% (vol/vol), and 2 mL of 0% (vol/vol) Percoll dissolved in isotonic isolation medium]. After centrifugation at 18,000 × *g* for 60 min in a swinging-bucket rotor, the fraction at the 25% Percoll interface was dissolved in sucrose-free isotonic isolation medium containing 500 mM n-octyl-β-D-glucopyranoside for 30 min on ice and then layered on a 0.5 mL 10% Percoll dissolved in sucrose-free isotonic isolation medium. After centrifugation at 8,000 × *g* for 30 min, dividing-peroxisome fraction was located at bottom pellet. This fraction was washed once with sucrose-free isotonic isolation medium by centrifugation at 700 × *g* for 20 min. The isolated dividing peroxisomal fraction was resuspended in sucrose-free isotonic isolation medium at a concentration of 1 mg of total protein per milliliter.

Proteomic Analysis of Dividing-Peroxisome Fraction. Samples were analyzed by a peptide mass fingerprinting search using a MALDI-TOF mass spectrometer AXIMA-TOF^2 (Shimadzu) in reflectron mode. Database searches were performed using the software program MASCOT Version 2.2.01 (Matrix Science) running on the local server against the *C. merolae* genome database (including 5,014 sequences), based on the FASTA file distributed by the *Cyanidioschyzon merolae* Genome Project (http://merolae.biol.s.u-tokyo.ac.jp) (1, 3). The permissible value of missed cleavages was set at one. Identified proteins with a MASCOT score greater than 50 are shown in Table S1.

Immunological Analysis. For immunoblotting, 20 μg of total protein extract from *C. merolae* was separated on 12.5% SDS/polyacrylamide gels and then transferred onto polyvinylidene difluoride membranes. After blocking with 5% skim milk in Triton X-100 Tris-buffered saline (TTBS), the membranes were incubated with primary antibodies: anti-Dnm1 rabbit antibody (4) (1:1,000 dilution), anti-catalase rat antibody (5) (1:2,000 dilution), anti-porin guinea pig antibody (6) (1:1,000 dilution), anti-mitochondrial-dividivision apparuts 1 (Mda1) mouse antibody (7) (1:1,000 dilution), and anti-plastid-division ring 1 (PDR1) rat antibody (8) (1:500 dilution) in TTBS. Alkaline phosphatase-conjugated goat anti-rabbit, rat, mouse, or guinea pig IgG was used at a dilution of 1/1,000 as the secondary antibody. Signals were detected using an alkaline phosphatase (AP) conjugate substrate kit (Bio-Rad). For immunofluorescence microscopy, cells were fixed and blocked as described previously with minor modifications (9). As primary antibodies, we used anti-Dnm1 rabbit antibody (1:200 dilution), anti-catalase rat antibody (1:500 dilution), anti-porin guinea pig antibody (1:500 dilution), anti-Mda1 mouse antibody (1:200 dilution), anti-filamentous-temperature sensitive Z1 (FtsZ) mouse antibody (10) (1:500 dilution), and anti-Dnm2 rabbit antibody (11) in PBS. As secondary antibodies, we used Alexa Fluor 488 or Alexa Fluor 555 goat anti-rabbit, anti-mouse, or anti-rat IgG (1:1,000 dilution). Images were captured using a fluorescence microscope BX51 (Olympus). Isolated peroxisome-dividing (POD) machineries were left unfixed in PBS. Primary antibody reactions were performed for 1 h at 37 °C with rabbit anti-Dnm1 diluted 1:1,000 in PBS. For the secondary antibody reactions, the primary antibodies were detected with Alexa Fluor 488 goat anti-rabbit IgG for 1 h at 4 °C. For microfluorometry, the intensity of fluorescence was quantified using a video-intensified microscope photon-counting system as described previously with minor modifications (12). The relative fluorescence intensity of particles and dynamin rings of dynamin-like protein Dnm1 were calculated at each sampling time. The signal intensity ratio of Dnm1 was calculated based on signal intensities of the whole rings.

Isolation of POD Machinery. The isolated dividing-peroxisome fraction was dissolved in peroxisome membrane dissolution buffer (PBS containing 2% wt/vol Nonidet-P40, 3 mM sodium lauryl sulfate, 10 mM urea) and incubated at 4 °C for 2 min. Isolation of the plastid-dividing (PD) ring was performed as described previously (13).

Negative Staining and Immunoelectron Microscopy. The fraction containing POD machineries with the peroxisome membrane, which was insoluble after 0.5% triton X-100 treatment, was left unfixed. Primary antibody reactions were performed for 1 h at 4 °C with anti-Dnm1 (diluted 1:10 in PBS), followed by a secondary reaction for 1 h at 37 °C with goat anti-rabbit IgG conjugated with 15-nm colloidal gold (diluted 1:10; British BioCell International). For double labeling, anti-dynamin reacted samples were incubated with anti-catalase (diluted 1:200 in PBS), followed by a secondary reaction with goat anti-rat IgG conjugated with 10-nm colloidal gold (diluted 1:10; British BioCell International). Then, samples were incubated in PBS containing 3 mM sodium lauryl sulfate and 10 mM urea for 15 min on ice, and the lysates were negatively stained with 0.5% phosphotungstic acid (pH 7.0). Samples were examined using an electron microscope (model JEM-1200; JEOL) (8). The labeling density of catalase and Dnm1 at each site was quantified using an ImageJ as described previously (4).

Plasmid Construction and Transformation. The plasmids which encode GFP targeted to mitochondria (pMtGFP and pMt GFP-Dnm1AS) were used in the antisense suppression assay of *Dnm1*. To construct pMtGFP, the promoter region (780 bp) and 5′ portion (220 bp) of the elongation factor-Tu (EF-Tu) gene (CMS502C), which includes a mitochondrial transit peptide, was amplified from *C. merolae* genomic DNA with the primers 5′- cgcGGATCCtga-

agtggcgagatcgtcgc-3′ (BamHI site is capitalized) and 5′- gcgcAGATCTgcgtttgcttgcactcgcct-3′ (BglII site is capitalized) in 25 cycles (98 °C for 10 s, 60 °C for 30 s, and 72 °C for 1 min) using PrimeSTAR HS DNA polymerase (TaKaRa Bio). The amplified fragment (1,000 bp) was digested with BamHI and BglII (TaKaRa Bio) and inserted into the BamHI site of pTH2PL[35] to make pMtGFP. To create a *Dnm1* antisense suppression construct regulated by the *Dnm1* promoter, the *Dnm1* promoter–*Dnm1* antisense-fused DNA fragment was amplified by overlap extension PCR. To obtain the antisense strand of the *Dnm1* ORF adjacent to the promoter region, the promoter region and the antisense strand of the *Dnm1* ORF were amplified individually. Using the oligonucleotide primers *Dnm1*_PromF_HindIII (5′-gcgcAAGCTTttcctccattctttcaaag-3′; HindIII site is capitalized) and *Dnm1*prom_reverse (R) (5′-ttcacgtcaaagaggagattgaagcctgtcgcgttcgccc-3′; overlapped sequence is underlined) and *C. merolae* DNA as a template, the promoter region of the Dnm1 gene (1,064 bp) was amplified. PCR was carried out for 30 cycles (98 °C for 10 s, 55 °C for 5 s, and 68 °C for 1 min) with PrimeSTAR HS DNA polymerase (TaKaRa Bio). Similarly, the antisense strand of the *Dnm1* ORF (2,304 bp) was amplified using the oligonucleotide primers *Dnm1*ASORF_forward (5′-gggcgaacgcgacaggcttcaatctcctctttgacgtgaa-3′; overlapped sequence underlined) and *Dnm1*ASORF_R (5′-catTCTAGAatggagcgcctaatacctatc-3′; XbaI site capitalized). Amplified fragments of the *Dnm1* promoter region and the antisense strand of the *Dnm1* ORF were separated by electrophoresis and purified using the QIAquick Gel Extraction kit (QIAGEN). PCR (98 °C for 10 s, 60 °C for 5 s, and 68 °C for 3.5 min) was performed with these fragments without template for 10 cycles to make a fused DNA fragment (3,387 bp). Then, using the fused fragment as a template, PCR was carried out with the primers *Dnm1*_PromF_HindIII and *Dnm1*ASORF_R for 20 cycles (98 °C for 10 s, 55 °C for 5 s, and 68 °C for 3.5 min) to amplify a DNA fragment of the antisense strand of the *Dnm1* ORF adjacent to the promoter region. The amplified fragment was digested with HindIII and XbaI and substituted for the HindIII-XbaI fragment of pMtGFP to make pMtGFP-Dnm1AS. The resultant plasmids, pMtGFP (control) and pMtGFP-Dnm1AS (for antisense suppression of *Dnm1*), contained an *EF-Tu* transit peptide–sGFP sequence driven by the *EF-Tu* promoter; therefore, transformed cells could be detected by green fluorescence under a fluorescence microscope.

Transformation of *C. merolae* cells was performed as described previously (14) with minor modifications. Cells were collected 24 h after introduction of DNA, transferred to new modified Allen's 2 medium, and then incubated for another 24 h.

1. Matsuzaki M, et al. (2004) Genome sequence of the ultrasmall unicellular red alga *Cyanidioschyzon merolae* 10D. *Nature* 428(6983):653–657.
2. Suzuki K, et al. (1994) Behavior of mitochondria, chloroplasts and their nuclei during the mitotic cycle in the ultramicroalga *Cyanidioschyzon merolae*. *Eur J Cell Biol* 63(2): 280–288.
3. Nozaki H, et al. (2007) A 100%-complete sequence reveals unusually simple genomic features in the hot-spring red alga *Cyanidioschyzon merolae*. *BMC Biol* 5:28.
4. Nishida K, et al. (2003) Dynamic recruitment of dynamin for final mitochondrial severance in a primitive red alga. *Proc Natl Acad Sci USA* 100(4):2146–2151.
5. Ohnuma M, et al. (2009) Transient gene suppression in a red alga, *Cyanidioschyzon merolae* 10D. *Protoplasma* 236(1-4):107–112.
6. Fujiwara T, Yoshida Y, Kuroiwa T (2009) Synchronization of cell nuclear, mitochondrial and chloroplast divisions in the unicellular red alga *Cyanidioschyzon merolae*. *Cytologia (Tokyo)* 74(1):1–2.
7. Nishida K, Yagisawa F, Kuroiwa H, Yoshida Y, Kuroiwa T (2007) WD40 protein Mda1 is purified with Dnm1 and forms a dividing ring for mitochondria before Dnm1 in *Cyanidioschyzon merolae*. *Proc Natl Acad Sci USA* 104(11):4736–4741.
8. Yoshida Y, et al. (2010) Chloroplasts divide by contraction of a bundle of nanofilaments consisting of polyglucan. *Science* 329(5994):949–953.
9. Nishida K, et al. (2004) Triple immunofluorescent labeling of FtsZ, dynamin, and EF-Tu reveals a loose association between the inner and outer membrane mitochondrial division machinery in the red alga *Cyanidioschyzon merolae*. *J Histochem Cytochem* 52(7):843–849.
10. Takahara M, et al. (2000) A putative mitochondrial *ftsZ* gene is present in the unicellular primitive red alga *Cyanidioschyzon merolae*. *Mol Gen Genet* 264(4): 452–460.
11. Miyagishima SY, et al. (2003) A plant-specific dynamin-related protein forms a ring at the chloroplast division site. *Plant Cell* 15(3):655–665.
12. Imoto Y, et al. (2010) Division of cell nuclei, mitochondria, plastids, and microbodies mediated by mitotic spindle poles in the primitive red alga *Cyanidioschyzon merolae*. *Protoplasma* 241(1-4):63–74.
13. Yoshida Y, et al. (2006) Isolated chloroplast division machinery can actively constrict after stretching. *Science* 313(5792):1435–1438.
14. Ohnuma M, Yokoyama T, Inouye T, Sekine Y, Tanaka K (2008) Polyethylene glycol (PEG)-mediated transient gene expression in a red alga, *Cyanidioschyzon merolae* 10D. *Plant Cell Physiol* 49(1):117–120.

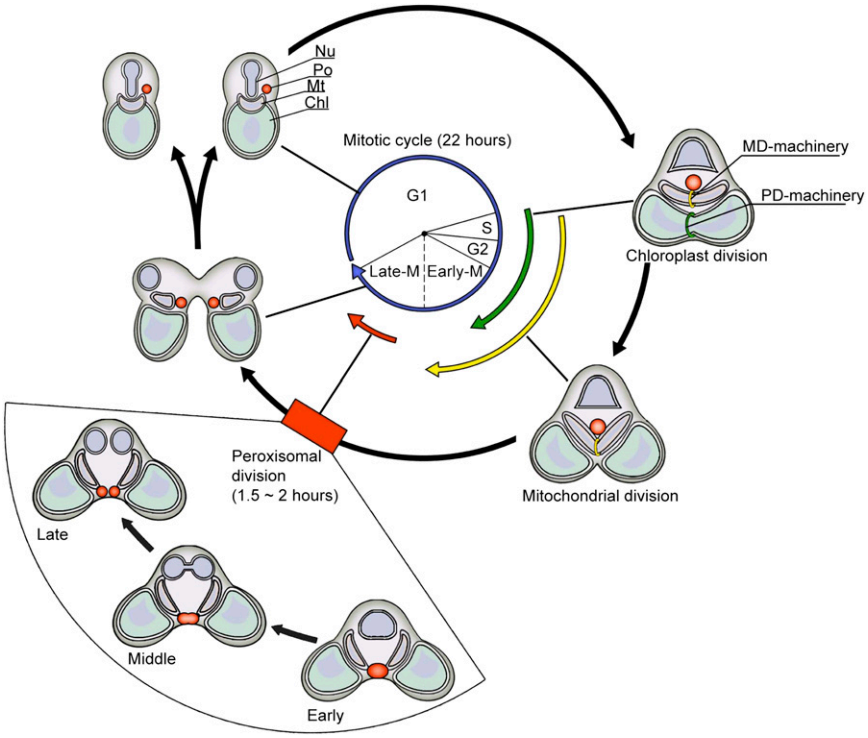

Fig. S1. Schematic representation of the timing of chloroplast, mitochondrial, and peroxisomal divisions during the cell cycle. The duration of the mitotic cycle of *C. merolae* is ~22 h. The chloroplast, mitochondrion, cell nucleus, and peroxisome divide in that order. Chloroplast (green arrow) and mitochondrial (yellow arrow) divisions occur during S–G_2 phase and early M phase (prophase). Peroxisomal division (1.5–2 h) (red arrow) occurs during late M phase (anaphase) after mitochondrial division. Oval-shaped peroxisomes become dumbbell-shaped from the early to middle periods of the division and finally divide into two daughter peroxisomes by binary fission. Chl, chloroplast; Mt, mitochondrion; Nu, cell nucleus; Po, peroxisome.

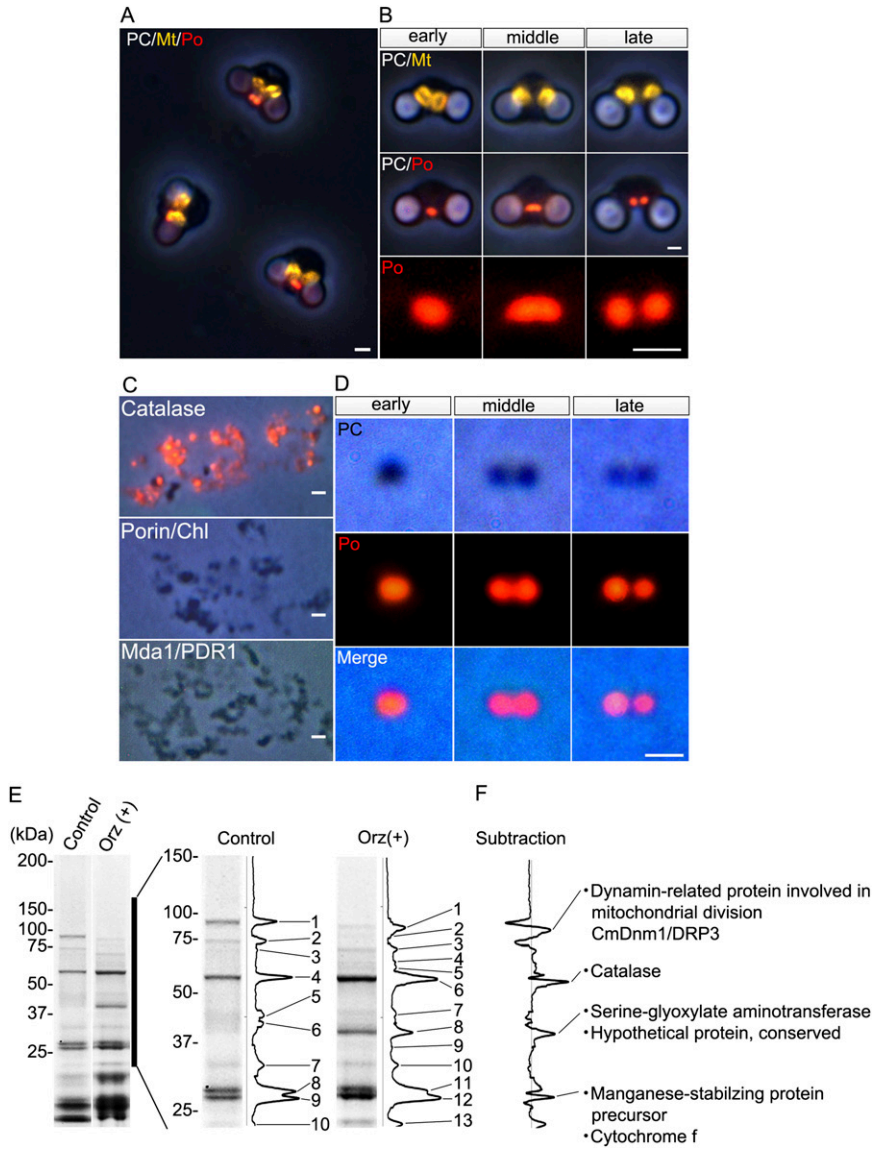

Fig. S2. Isolation and proteomic analysis of peroxisomal fractions. (*A*) Phase-contrast and immunofluorescence images of oryzalin-treated cells. At 20 h after the onset of synchronization, the oryzalin-treated culture contains many divided mitochondria (yellow, anti-porin) and dividing peroxisomes (red, anti-catalase). (*B*) Phase-contrast and immunofluorescence images of peroxisomal divisions in oryzalin-treated cells. In the oryzalin-treated cells, divisions of peroxisomes (red, anti-catalase) occur in the same manner as in control cells. (*C*) Phase-contrast (PC) and immunofluorescence images of peroxisomes (red, anti-catalase) in the dividing peroxisomal fraction. Mitochondria (anti-porin), chloroplast red autofluorescence (chl), mitochondrion-dividing (MD) machinery (anti-Mda1), and PD machinery (anti-PDR1) are not detected in this fraction. (*D*) Enlarged images of a dividing peroxisome (red, anti-catalase) in the dividing-peroxisomal fraction. (Scale bars: 1 μm.) (*E*) Proteins in the isolated peroxisomal fractions from control and oryzalin-treated cells (Orz+) at 20 h. The gel image on the right is an enlarged image of the left gel image (bar). Ten (control cells) and 13 (oryzalin-treated cells) bands are identified by MALDI-TOF mass spectrometry. The numbers of identified proteins are described in Table S1. (*F*) Major subtracting bands from those of the peroxisomal fractions in control and oryzalin-treated cells. The three major peaks are identified as CmDnm1/DRP3 (Dnm1), catalase, and serine-glyoxylate aminotransferase. Catalase and serine-glyoxylate aminotransferase are known to be peroxisomal proteins. Mt, mitochondrion; Po, peroxisome.

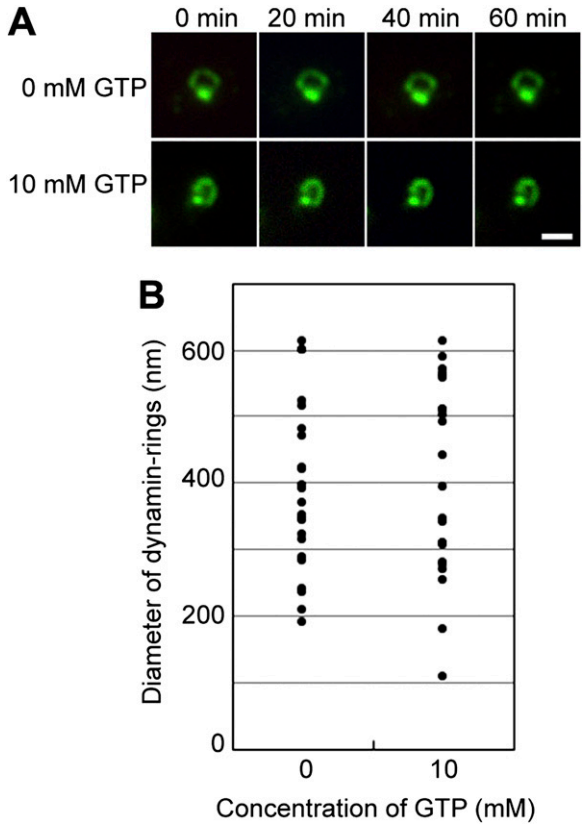

Fig. S3. Effect of GTP on isolated dynamin rings. (*A*) Immunofluorescence images of an isolated dynamin ring stained for Dnm1 (green, anti-Dnm1) taken every 20 min from 0 to 60 min after addition of 10 mM GTP. (Scale bar: 500 nm.) (*B*) Comparison of the populations of isolated dynamin rings before and after addition of 10 mM GTP ($n = 25$). A conformational change of the isolated dynamin ring is not induced by GTP addition.

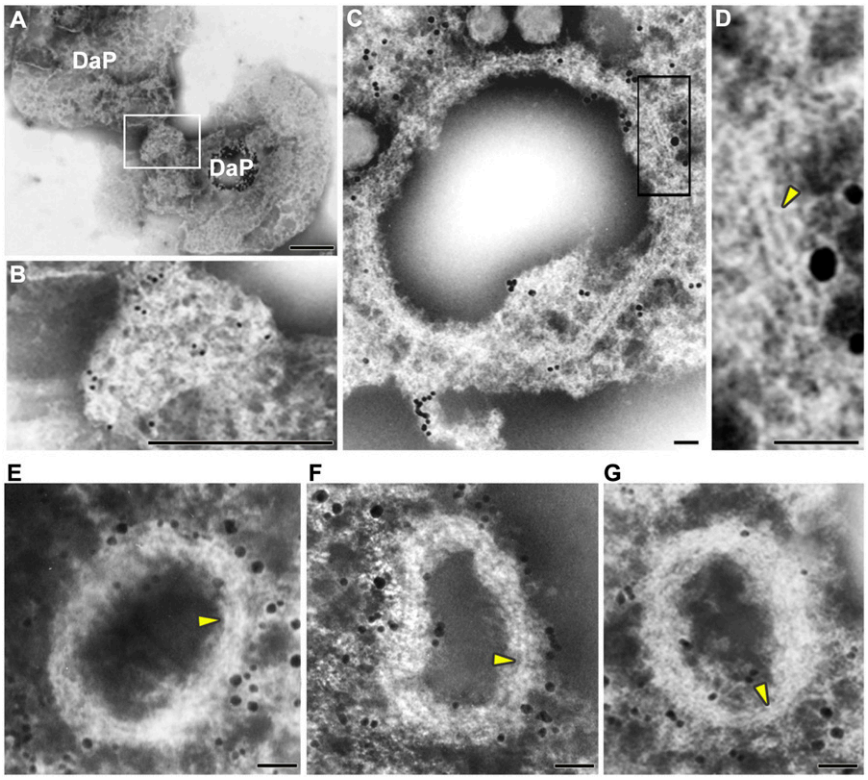

Fig. S4. Immunoelectron microscopic images of the isolated POD machinery. (*A* and *B*) The POD machinery is localized on a bridge between the daughter peroxisomes. The filamentous ring is covered by the dynamin-based ring. (*C* and *D*) When the membrane is dissociated or dissolved from the POD machinery, the filamentous ring of about 30 nm in width, which is a constituent of the POD machinery and consists of a bundle of fine filaments of about 6 nm in diameter (yellow arrowhead), appears. Dnm1 remains around the filamentous ring. (*E*–*G*) Even when the diameter of the POD machinery becomes small, the filamentous rings are bundles of filaments (yellow arrowheads). DaP, daughter peroxisomes; large immunogold particles (15 nm), Dnm1 (*A*–*G*); small immunogold particles (10 nm), catalase (*C*–*G*). *B* and *D* show enlarged micrographs of the boxed areas in *A* and *C*, respectively. (Scale bars: 50 nm.)

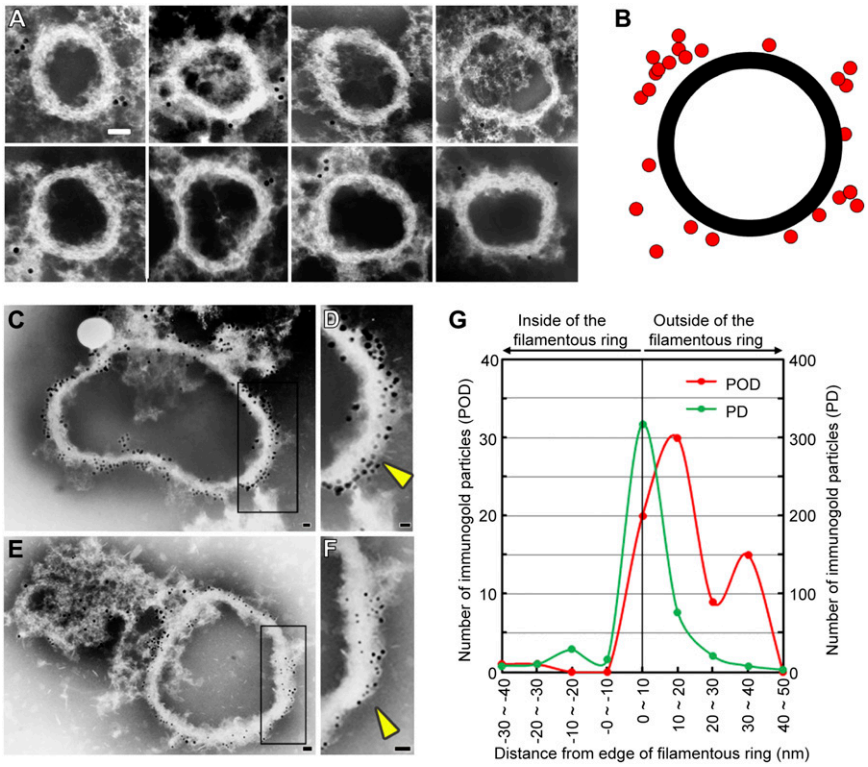

Fig. S5. Immunoelectron microscopic images of isolated POD and PD machineries and schematic representations showing the distributions of Dnm1 and Dnm2. (*A*) In the isolated POD machinery, a few Dnm1 signals remain around the filamentous rings even after detergent treatment for 5 min. (*B*) Scatterplot showing the distribution of immunogold particles (black dots) around the filamentous ring (blue ring) in a stacked pile of the isolated POD machinery shown in *A*. (*C*–*F*) In the isolated PD machinery, many Dnm2 signals are closely attached to the peripheral region of the filamentous rings (yellow arrowheads). (*G*) Distribution of Dnm1 on the POD machinery (red line) and Dnm2 on the PD machinery (green line). Dnm2 in the PD machinery is distributed closer to the filamentous rings than Dnm1 in the POD machinery. This may be why the dynamin-based ring in the POD machinery is easily peeled from the filamentous ring. POD, $n = 76$; PD, $n = 489$. Boxed areas, enlarged images; large immunogold particles (15 nm), Dnm1 (*A*) and Mda1 (*C*–*F*); small immunogold particles (10 nm), Dnm2 (*C*–*F*). *D* and *F* show enlarged micrographs of the boxed areas in *C* and *E*, respectively. (Scale bars: 50 nm.)

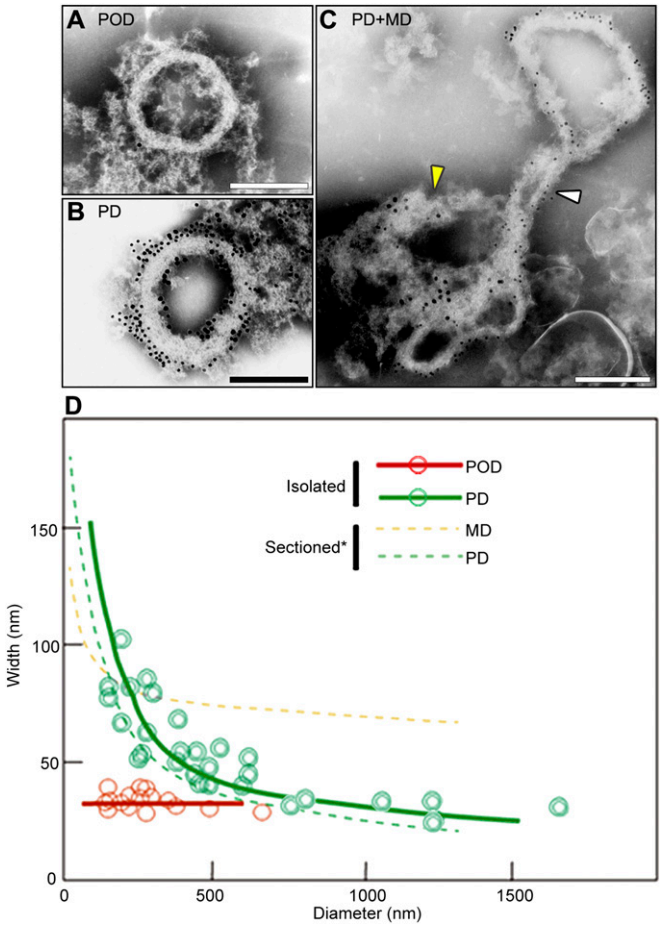

Fig. S6. Comparison of the structures among the POD, MD, and PD machineries. (*A*–*C*) Immuno-EM images of isolated POD, PD, and PD machineries (white arrowhead) with the MD machinery (yellow arrowhead), respectively. (*D*) Widths of the POD (red line), MD, and PD (green line) machineries versus the diameter of the organelles. Because the isolated MD machinery becomes irregular in shape, the diameter and width cannot be measured. Therefore, the data for thin sections of the MD and PD machineries are used (MD, dashed red line; PD, dashed green line). The diameters of sectioned and isolated PD machineries were measured. The POD machinery is smaller in width and diameter than the MD and PD machineries. Whereas the PD and MD rings become wider during contraction, the width of the POD machinery is constantly about 30 nm throughout contraction. Large immunogold particles (15 nm): Dnm1 (*A*), Dnm2 (*B*), and Mda1 (*C*); small immunogold particles (10 nm): FtsZ2 (*B*) and Dnm2 (*C*). (Scale bars: 200 nm.)

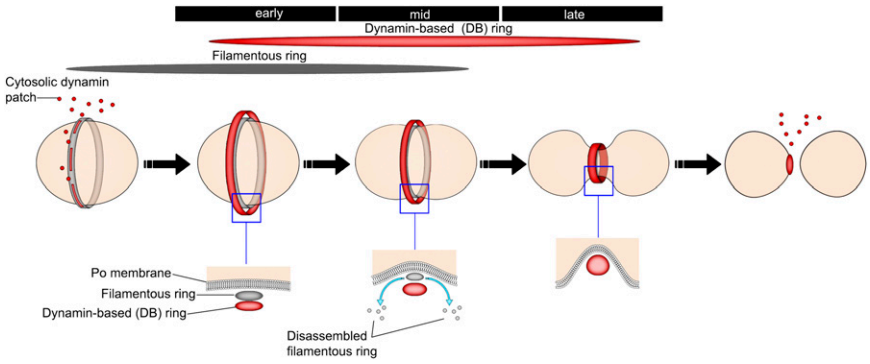

Fig. S7. Working model of Dnm1 function in the POD machinery during the contraction and pinching off of peroxisomes at the division site. The POD machinery consists of an outer dynamin-based ring (red) and an inner filamentous ring assembled on the cytosolic side of the peroxisome (Po) membrane. Dynamin-based ring (Dnm1 molecules and amorphous string) formed and encircles filamentous ring (Early). The dynamin-based ring generates contraction force for the POD machinery by sliding the filamentous ring at the division site of the peroxisome and partial digestion of the filamentous ring (Middle). The filamentous ring disassembles and then the single membrane bridge between the daughter peroxisomes is pinched off directly by the dynamin-based ring (Late). After division of the peroxisome, the dynamin molecules move to the cytosol.

Table S1. Proteomic analysis of isolated peroxisomal fraction at 20h in control and Oryzalin treated cells

Cells*	Locus	Annotation	Expect
Control cells			
1	**CMV157**	**[pt] phycobilisome linker polypeptide**	7.9E-13
2	CMQ054C	Hypothetical protein, conserved	0.00032
	CMA044C	Cryptochrome DASH	0.011
3	**CMH197C**	**Mitochondrial F-type ATPase F1 subunit β, precursor**	**0.00037**
	CMR087C	**Hypothetical protein, conserved**	**0.028**
4	CMI050C	Catalase †	0.0015
5	**CMV196C**	**ATP synthase CF1 β chain**	0.000004
6	ND		
7	**CMD067C**	**Probable prohibitin protein**	**0.0013**
	CML334C	**Hypothetical protein, conserved**	**0.0046**
	CMM221C	**Hypothetical protein**	**0.006**
8	CMV051C	Phycobilisome rod-core linker polypeptide	0.000016
9	**CMV155C**	**Cytochrome f**	**0.03**
10	ND		
Oryzalin-treated cells			
1	**CME019C**	**Dynamin-related protein involved in mitochondrial division CmDnm1/DRP3**	0.0066
2	CMI157C	ATP-dependent zinc protease	0.0023
3	**CMD101C**	**Unknown GTP-binding protein**	0.00021
	CMT273C	**Type II DNA topoisomerase VI subunit B**	**0.0053**
	CMH197C	**Mitochondrial F-type ATPase F1 subunit β, precursor**	**0.0085**
	CMQ241C	**Probable plastid-specific ribosomal protein PSRP-1 precursor**	**0.032**
4	CME141C	Similar to GTP-binding protein	0.035
	CMT322C	Chaperonin containing TCP1, subunit 2 (beta)	0.02
5	**CMQ295C**	**Cell division protein FtsH**	**0.0044**
	CMS291C	**Similar to FKBP-type peptidyl-prolyl cis-trans isomerase Mip**	**0.0096**
	CME103C	**Hypothetical protein, conserved**	**0.037**
	CML258C	**Hypothetical protein**	**0.051**
6	CMI050C	Catalase†	0.0000002
7	**CMO274C**	**V-type ATPase V0 subunit d**	**0.042**
8	CMS429C	Serine-glyoxylate aminotransferase†	0.00074
	CMT344C	Hypothetical protein, conserved	0.0047
9	**CMD105C**	**Similar to peroxisomal membrane protein PEX2†**	**0.011**
10	CMD067C	Probable prohibitin protein	0.0013
	CML334C	Hypothetical protein, conserved	0.0035
	CMS224C	Hypothetical protein, conserved	0.0045
11	**CML063C**	**Hypothetical protein**	0.000013
	CMV051C	**Phycobilisome rod-core linker polypeptide**	0.0016
12	CMI290C	Manganese-stabilizing protein precursor	0.00046
	CMV155C	Cytochrome f	0.0024
13	**CMN155C**	**Probable β-alanine synthase, closer**	**0.013**

Mascot scores higher than 50 are shown. Odd numbers are shown in bold. ND, not detected.
*The numbers coincide with the bands in Fig. S2*E*, respectively.
†Known peroxisomal proteins.

Table S2. Features of peroxisome-dividing (POD) machineries and comparison to mitochondrion-dividing (MD) and plastid-dividing (PD) machineries

	Organelle		
Feature	Peroxisome	Mitochondrion	Chloroplast
Whole organelle			
Membrane	Single	Double	Double
DNA	-	+	+
Diameter of division site (sectioned) (nm)	500 (250)	750 (730*)	1000 (1270*)
Division machinery	POD	MD	PD
Isolated machinery			
Structure			
Shape	Ring	Irregular	Ring
Diameter (nm)	150 – 600	150 – 1200†	150 – 1300†
Width (nm)	25 – 30	30 – 120	20 – 130
Supertwist	-	N. D.	+
Composition			
Filament (nm) (component)	4 – 5 (N. D.)	N. D.	5 – 7 (polyglucan)
Dynamin homolog	Dnm1	Dnm1	Dnm2
FtsZ homolog	-	FtsZ1-1, 1-2	FtsZ2-1, 2-2
Mdv1 homolog	N. D.	Mda1	N. D.
Glycosyltransferase	-	N. D.	PDR1

ND, not detected.

*The diameter of the MD ring was calculated by the circumference from ref. 8.

†Data for the diameters of the MD and PD rings are from ref. 8.